LIP-STUDENTS-20-05

The hidden charm in the COMPASS experiment at CERN

Catarina Corte-Real[1,a] and Francisco Feliciano[2,b]

[1] *Instituto Superior Técnico, Lisboa, Portugal*
[2] *Faculdade de Ciências da Universidade de Lisboa, Portugal*

Project supervisors: C. Quintans, M. Quaresma

October 2020

Abstract. This work is based in analysing the J/ψ particle, which is a meson composed by charm quarks, here studied in light of its decay in the form of two muons, detected in the COMPASS experiment. The data analysis requires event selection using the tracks' reconstruction parameters, resulting in only about 2% of the initial data being used. In this analysis the J/ψ particle is identified from the invariant mass of the muons pair, centered around 3.097 GeV/c^2, and its peak can be compared depending on the target material the particle originated from. The background under the J/ψ signal was also obtained, and was around 20%, in the region of interest. The transverse momentum also illustrates the differences between targets.

Keywords: COMPASS, J/ψ, dimuon invariant mass, charm quarks

1 Introduction

1.1 The COMPASS experiment

COMPASS (Common Muon and Proton Apparatus for Structure and Spectroscopy) is one of the experiments at CERN, and its main goals regard hadron spectroscopy and the study of nucleon spin structure. It is a fixed target experiment, at the M2 beam line of the SPS (Super Proton Synchrotron). In the 2018 (and 2015) data taking, the focus was on the measurement of the polarized Drell-Yan process. There was a 190 GeV negative charged pion beam, and two ammonia polarized targets, followed by two unpolarized targets made of aluminum and tungsten. The setup has a two-staged spectrometer and several detectors of different types to identify the particles and reconstruct their trajectories. There is also an hadron absorber, with the heavy tungsten target inside it, to clean the muon sample required for the analysis, excluding hadrons from passing this stage in the apparatus. Furthermore, there are two muon walls made of iron and concrete, with the similar purpose of identifying the particles which cross them as muons, since muons barely interact and can, therefore, pass such heavy barriers. The trigger system is made with hodoscope detectors (Outer, Middle and LAS sets), the first 2 in SAS (Small Angle Spectrometer), downstream in the spectrometer, and the third in LAS (Large Angle Spectrometer), closer to the target. The triggers used to select dimuons correspond to one muon hitting Middle (SAS) and other LAS (later referred to as trigger 0); one hitting Outer (SAS) and other LAS (later referred to as trigger 2) and both hitting LAS (later referred to as trigger 8) [1]. This setup is represented in Figure 1.

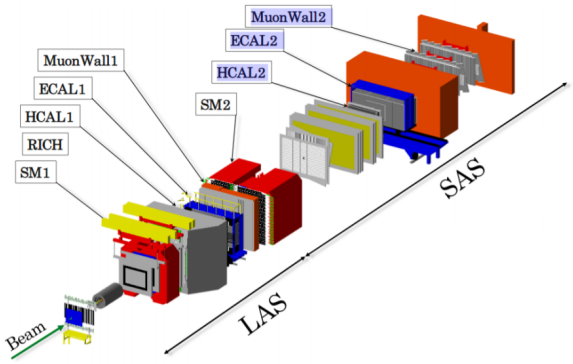

Figure 1. COMPASS setup in the Drell-Yan data taking (2015 and 2018)

1.2 J/ψ particle

The J/ψ particle, a meson of hidden charm, is composed by a charm quark-antiquark pair, so this meson is also known as Charmonium. This particle is the lightest $c - \bar{c}$ vector meson, with an invariant mass of 3.096900 ± 0.000093 GeV/c^2 [2], and it is represented in Figure 2.

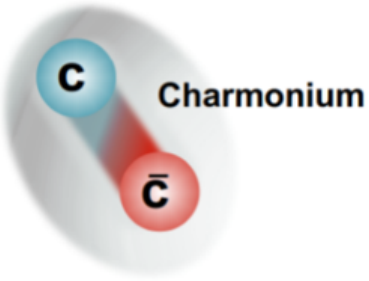

Figure 2. Representation of the J/ψ particle.

This meson has a mean lifetime of 7.2 zeptoseconds (7.2×10^{-21} s), which means that it is a short lived particle.

[a] e-mail: catarina.corte-real@tecnico.ulisboa.pt
[b] e-mail: franciscofeliciano99@hotmail.com

Among other decays, the one resulting in a pair of muons of opposite charge is possible to detect in the COMPASS experiment. There are two processes to create the J/ψ particle (illustrated in Figure 3), one is the quark anti-quark annihilation, in which a quark is provided from the target, the anti-quark is from the beam, and their interaction initiates the production mechanism, creating the hidden charm. The other process is the gluon-gluon fusion, with one of the gluons originating from the beam and the other one from the target, creating the J/ψ particle.

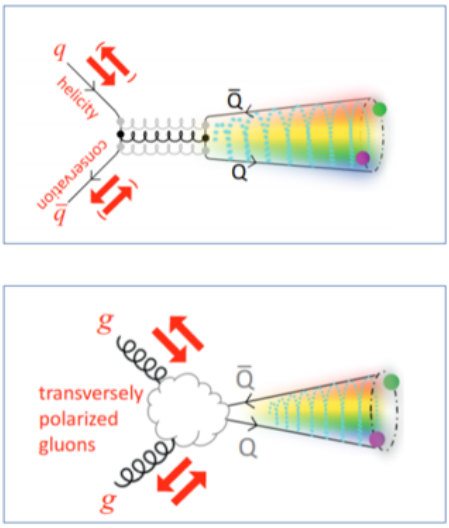

Figure 3. Two mechanisms of J/ψ production.

2 Spectrometer angular acceptance

LAS and SAS have different angular acceptances. The muons' polar angle with respect to the beam trajectory, θ, is shown in Figures 4 and 5 for each of these spectrometers. Particles hitting LAS have θ between about 20 and 250 mrad, whereas for particles hitting SAS it is less than 100 mrad.

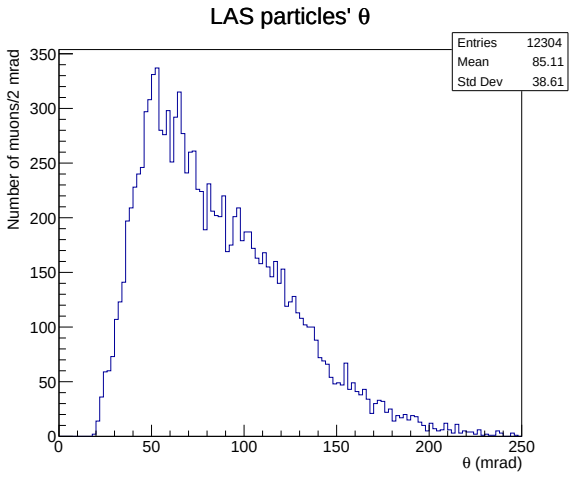

Figure 4. θ of the muons that hit LAS.

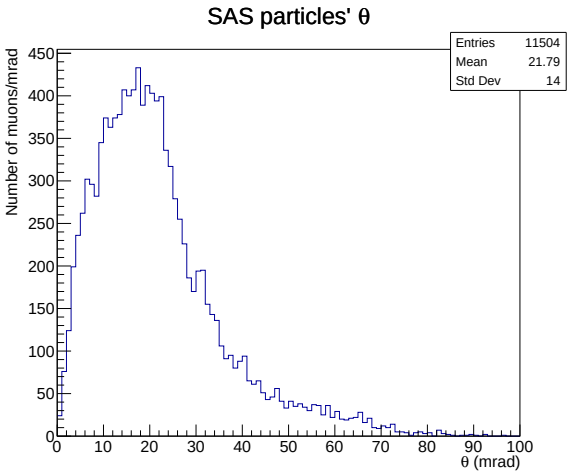

Figure 5. θ of the muons that hit SAS.

3 Event selection using *PHAST* and ROOT

The *PHAST* software [3] is the data analysis package providing direct access to the properties of the reconstructed trajectories of the particles, including the vertex (primary or not) and the particles' properties themselves. Two runs of the 2018 Drell-Yan COMPASS data were used for this study.

To analyse the properties of the J/ψ particle, a selection of events with at least one dimuon on the final state was necessary. *PHAST* was therefore used to make this selection, as listed below in table 1.

Table 1. Criteria for event selection.

Cut's name	Variable	
	iBestCoralPrimaryVertex()	
	Particles' PID	5 or 6
TD	Time difference between two muons	< 5 ns
PMT	Particles' mean time	< 10 ns
χ^2/nDF	Track's χ^2/nDF	< 10
Z_{low}	Z_{vertex}	>-350 cm
Z_{high}	Z_{vertex}	<120 cm
Z_{first}	Z_{first}	<300 cm
Z_{last}	Z_{last}	>1500 cm
$Radius^2$	$X_{vertex}{}^2$+$Y_{vertex}{}^2$	< 4 cm^2
	Trigger bit	0 or 2 or 8

With these cuts, one selects successfully reconstructed particles, compatible with a muon-antimuon pair candidate (PID 6 and 5, respectively), with time difference between them not too large (TD), and rejecting the ones which deviate more than 10ns (PMT). Particles' tracks were also selected with a χ^2/nDF below 10. Z_{low} and Z_{high} are only preliminary, since in further analysis the dimuons will be separated by target. Z_{first} is the z-position in which the first hit on a detector happened, here forced to happen before crossing SM1, the first magnet, and Z_{last} is the z-position in which the last hit on a detector happened, forced to be after the first muon wall. Only the particles with vertices located within a 2 cm radius to the center in

the plane parallel to the targets are considered, and only dimuon triggers are selected, according to section 1.1.

These cuts reduced the sample of dimuons to about 2% of its previous size, the reduction being predominantly in the $M < 2.5$ GeV/c^2 region, therefore cleaning some background, as shown in Figure 6. The cuts made also enhance the Z position of the vertex in which the dimuons were formed, since the different target cells become more distinguishable when the sample is cleaned, as can be seen in Figure 7. One can also understand the effect of different mass cuts. Only the selected events with $M > 2$ GeV/c^2 were used in the analysis that follows.

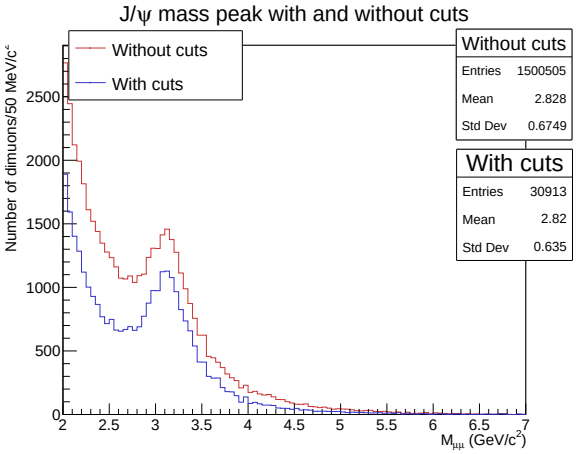

Figure 6. Invariant mass of the dimuons with and without event selection.

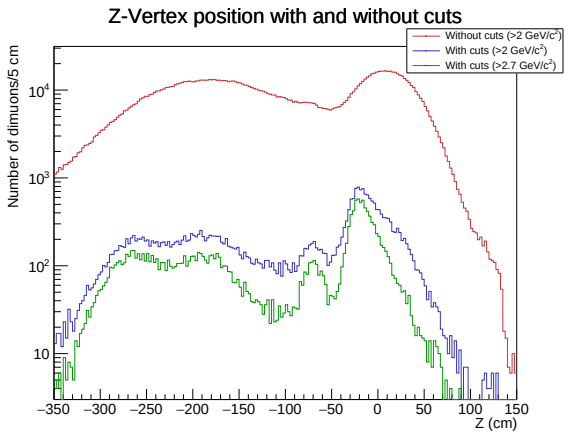

Figure 7. Dimuons Z vertex distributions with and without event selection.

4 Results

4.1 Dimuon invariant mass per target

The invariant mass distribution gives information about the process through which the dimuons were created. The J/ψ peak appears much larger than its physical width, some keV according to the PDG, due to the experimental finite resolution, that varies depending on the target material the dimuon was produced in. The invariant mass distribution was produced for different targets to study the J/ψ peak in more detail. This distribution was fitted considering a background in the form of a decreasing exponential, e^{a+bx}, b<0, and the mass peak to be gaussian. This expression for the background is not the most rigorous, since the background is a sum of components of different origins, such as random combinations of opposite charge muons, the decay of two D mesons, the Drell-Yan process, and the ψ' direct decay to a pair $\mu^+\mu^-$. One single gaussian to fit the mass peak is also not that good when more statistics are included. In conclusion, the use of this simplified fit function is only possible since only two runs of data were used. The statistical error is large enough that the few free parameters of the fit function are able to describe it.

4.1.1 NH_3 target

For dimuons produced in the NH_3 target ($-294.5 < Z_{vertex} < -239.4$cm or $-219.5 < Z_{vertex} < -163.9$ cm), the σ was the smallest, since this is the lighter material, where pion beam and outgoing muons suffer the least multiple scattering. The average value of the peak in the J/ψ region is 3.13 GeV/c^2, which differs from the PDG value because of the contribution of the background, and due to smearing. The χ^2/nDF is about 1.47, which considering the previous reasons, is not too large. This distribution is in Figure 8.

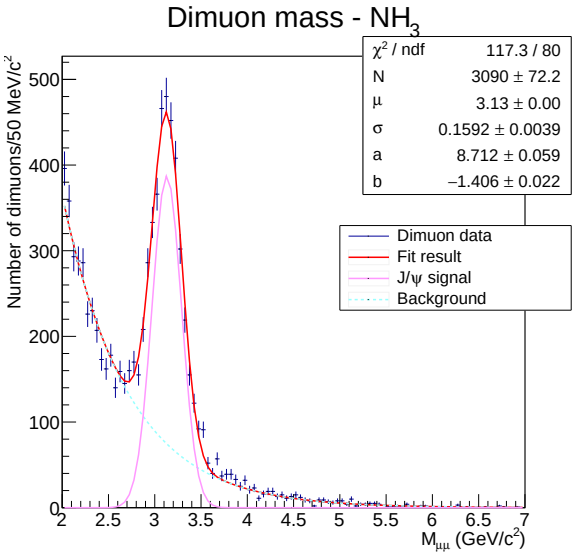

Figure 8. Dimuon invariant mass for the NH_3 target.

4.1.2 Aluminum target

Since this target is the shortest, only 7 cm long (but selecting $-80 < Z_{vertex} < -60$ cm, to recover part of the events smeared out), and also light, the number of J/ψ particles is smaller, as can be seen in Figure 9. The J/ψ mass value, μ=3.095 ± 0.015 GeV/c^2 agrees with the PDG value, and the χ^2/nDF is only a little under 1.

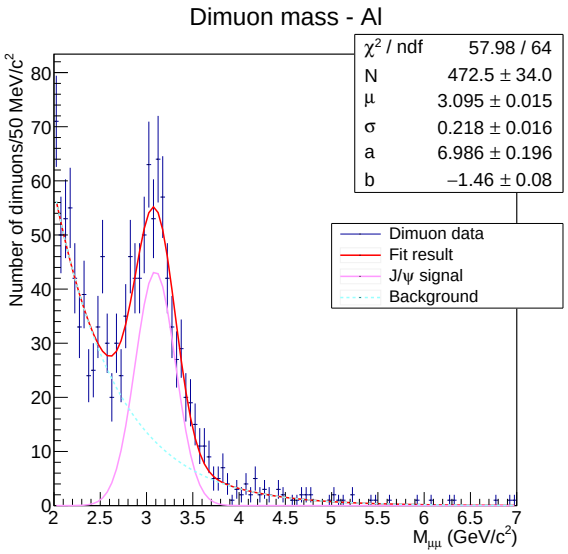

Figure 9. Dimuon invariant mass for the aluminium target.

4.1.3 Tungsten target

Since the tungsten target is heavy, the beam particles which have not interacted yet when they get to this Z position are likely to do so. The selection $Z_{vertex} > -40$ cm is applied, that recover events smeared out, up to 10 cm upstream of the nominal target position. That explains the amount of J/ψ events in the first 20cm of this target being nearly as large as the ones produced in NH_3. It also explains the width of the invariant mass peak, shown in Figure 10, larger since pion beam and muons suffer from higher multiple scattering in this material. The invariant mass value for the J/ψ particle is μ=3.198 ± 0.008 GeV/c^2, which agrees with what was expected, and the χ^2/nDF is about 1.24.

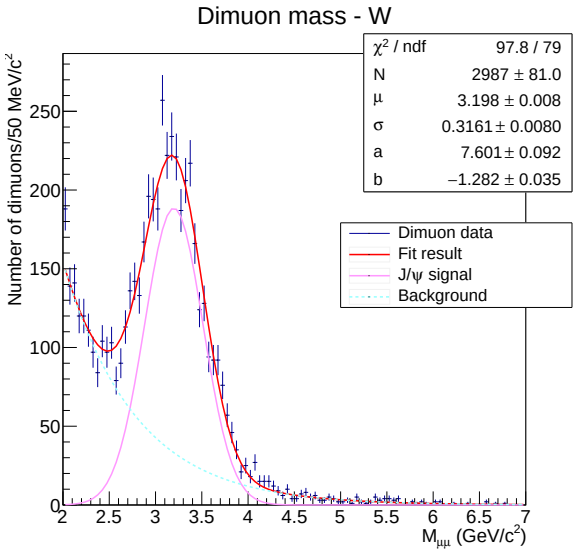

Figure 10. Dimuon invariant mass for the tungsten target.

4.2 Signal and background

The preceding analysis allowed for the calculation of the background in the J/ψ invariant mass region (mass pole $\pm1\sigma$), using ROOT's integral function.

Table 2. Background percentage in the J/ψ invariant mass region (mass pole $\pm1\sigma$) for each target.

Target	Background (%)	Mass range (GeV/c^2)
NH_3	18.5 ± 4.1	[3.0, 3.3]
Aluminium	24.5 ± 11.9	[2.9, 3.3]
Tungsten	17.5 ± 4.1	[2.9, 3.5]

These values, presented in table 2, are still relatively large, which is justified by the cuts made in the sample being only preliminary, and the fitting functions not being the best, as explained in section 4.1. Further analysis would require more effective cuts, and therefore smaller background percentages. However, these background values are already smaller than the ones obtained in table 3, which shows how the fraction of J/ψ signal is affected as each selection cut is excluded.

Table 3. Impact of each cut when applied on top of the others.

Excluded cut	Total entries (2 to 7 GeV/c^2)	Total entries in J/ψ region (J/ψ pole $\pm1\sigma$)	Total J/ψ (in the region $\pm1\sigma$) (%)	Total Bck (in the region $\pm1\sigma$) (%)
None	30913 ± 176	8552 ± 92	67.6 ± 5.1	32.4 ± 3.2
TD	37681 ± 194	8720 ± 93	61.3 ± 4.5	38.7 ± 3.3
PMT	30943 ± 176	8553 ± 92	67.5 ± 5.1	32.5 ± 3.2
χ^2/nDF	31077 ± 176	8552 ± 92	67.4 ± 5.1	32.6 ± 3.2
$Radius^2$	34621 ± 186	9158 ± 96	65.2 ± 4.7	34.8 ± 3.1
Z_{low}	31192 ± 177	8628 ± 93	67.7 ± 5.1	32.3 ± 3.1
Z_{high}	30915 ± 176	8551 ± 92	67.6 ± 5.1	32.4 ± 3.2
Z_{first}	31012 ± 176	8553 ± 92	67.5 ± 5.1	32.5 ± 3.2
Z_{last}	30977 ± 176	8578 ± 93	67.6 ± 5.1	32.4 ± 3.1

In table 3, there are the number of dimuons (total entries) with masses between 2 and 7 GeV/c^2, the number of dimuons in the J/ψ invariant mass region (mass pole $\pm1\sigma$), as well as the fraction of J/ψ estimated in this region and its background percentage. In the first line, all cuts mentioned in section 3 are considered, so these numbers serve as a reference to study the impact of each cut. The same quantities were calculated for the same sample excluding each of them at a time. One can hence see their importance, since the J/ψ fraction in the region of interest is always lower (within the error interval) when a cut is removed. The cut with greater impact is then thought to be the one regarding the time difference between particles (TD), since the total background without this cut being made is the largest.

This analysis was made without distinguishing the dimuons by the material they originated from, so it is not completely rigorous, because, as seen in subsection 4.1, the invariant mass J/ψ peak's width depends on the target material. However, it was made to roughly understand the importance of the cuts.

4.3 Dimuon transverse momentum in the J/ψ range

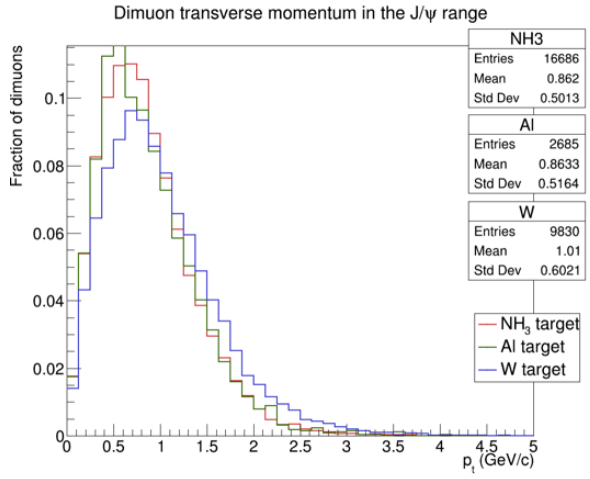

Figure 11. Dimuon transverse momentum in the J/ψ range.

To further understand properties of the J/ψ particle, its transverse momentum is considered. As expected, the transverse momentum grows as the material's heaviness gets larger, due to nuclear effects, which can be seen in the average values of the p_t in Figure 11. The width of the p_t distribution also varies depending on the target material, being wider for tungsten, since the p_t values are larger for this target, comparing with the other two.

5 Conclusions

With the selection of events made, the J/ψ invariant mass peak, centered around 3.097 GeV/c^2, was analysed, and its properties were found to be dependent on the target, as expected. The heavier the target material in which the production of the J/ψ particle occurs, the more scattering will happen, and, therefore, the larger the peak's width is going to be. With the cuts made, which were only preliminary, the background was found to be around 20%, in the region of the mass pole $\pm 1\sigma$. COMPASS collected a very large sample of J/ψ events during the 2018 data taking. For this paper, however, only about 2 hours of this data were used, from which stems some statistical imprecision which would be reduced with the analysis of a larger sample. In fact, summing over all targets, there were only about 6550 J/ψ in this study. Lastly, for further analysis on this topic some additional kinematic properties of this particle could be studied, such as the Feynman x distribution, in order to gain more insight about its mechanisms of production.

Acknowledgements

The authors of this paper would like to thank their project supervisors, Catarina Quintans and Márcia Quaresma, for their support, their availability and the enthusiasm for the subject, with which they guided us through this project.

References

[1] *Compass*, https://wwwcompass.cern.ch (2020), [Online]

[2] P.D. Group, https://pdg.lbl.gov/index.html (2020), [Online]

[3] *Phast*, http://ges.web.cern.ch/ges/phast/index.html (2020), [Online]